Regular Article

Geochemistry, Geophysics, Geosystems
DOI 10.1002/jgrc.20205

AVHRR, MODIS, and VIIRS Radiometric Stability and Consistency in SST Bands

XingMing Liang[1,2], Alexander Ignatov[1]

[1] *NOAA/NESDIS, Center for Satellite Application and Research (STAR), College Park, MD 20740*

[2] *CSU, Cooperative Institute for Research in the Atmospheres (CIRA), Fort Collins, CO 80523*

**Corresponding author address: XingMing Liang, NOAA/NESDIS/STAR, NCWCP, College Park, MD 20740; e-mail: Xingming.Liang@noaa.gov*

Accepted Article

This article has been accepted for publication and undergone full peer review but has not been through the copyediting, typesetting, pagination and proofreading process which may lead to differences between this version and the Version of Record. Please cite this article as doi: 10.1002/jgrc.20205

© 2013 American Geophysical Union

Received: Jan 29, 2013; Revised: Apr 16, 2013; Accepted: Apr 17, 2013

ABSTRACT

Monitoring of IR Clear-Sky Radiances over Oceans for SST (MICROS; www.star.nesdis.noaa.gov/sod/sst/micros) is NESDIS near-real time web-based radiance monitoring system. It analyzes Model (Community Radiative Transfer Model, CRTM) minus Observation (M-O) biases in brightness temperatures (BT) in three bands centered at 3.7 (IR37), 11 (IR11), and 12µm (IR12), for several AVHRR (NOAA-16, -17, -18, -19, Metop-A, -B), VIIRS (Suomi National Polar Partnership, S-NPP), and MODIS (Terra, Aqua) sensors. Double-differences (DD) are employed to check BTs for radiometric stability and consistency. All sensors are stable, with the exception of two AVHRRs, onboard NOAA-16 and to a lesser extent NOAA-18, and generally consistent. VIIRS onboard S-NPP, launched in October 2011, is well in-family, especially after its calibration was fine-tuned on 7 March 2012. MODIS M-O biases were initially out-of-family by up to -0.6 K, due to incorrect CRTM transmittance coefficients. Following MICROS feedback, CRTM Team updated coefficients and brought MODIS back in-family. Terra and Aqua BTs are very consistent in IR11 and IR12 but show cross-platform bias of 0.3 K in IR37, likely attributed to MODIS characterization. Work with MODIS Characterization Support Team is underway to resolve this. Initial analyses of AVHRR onboard Metop-B launched in September 2012 suggest that its BTs are offset from Metop-A by up to ~0.3 K. Overall, MICROS DDs are well suited to evaluate the sensors stability, but dedicated effort is needed to ensure consistent radiative transfer modeling (RTM) calculations for various sensors before DDs can be used in Global Space-based Inter-Calibration System (GSICS) quantitative applications.

Accepted Article

1. Introduction

The Joint Polar Satellite System (JPSS) is the follow-on to the current NOAA Polar Orbiting Environmental Satellite (POES) and NASA Earth Observing System (EOS). The Suomi National Polar-orbiting Partnership (S-NPP) satellite launched on 28 October 2011 is the bridge between the POES/EOS and JPSS. S-NPP and follow-on JPSS satellites are flown in an afternoon orbit (1:30 am/pm), whereas the European Organization for the Exploitation of Meteorological Satellites (EUMETSAT) contributes Meteorological Operational (Metop) satellites in a mid-morning (10:30 am/pm) orbit. Metop-A was launched on 19 October 2006 and as of this writing, continues operating well. On 17 September 2012, Metop-B was launched; its performance is also nominal. NOAA and Metop satellites carry the Advanced Very High Resolution Radiometer (AVHRR), whereas EOS satellites, Terra and Aqua, carry the Moderate Resolution Imaging Spectroradiometer (MODIS), and S-NPP/JPSS carry the Visible Infrared Imaging Radiometer Suite (VIIRS). NOAA, in conjunction with its partners, is responsible for the full suite of radiances (Sensor Data Records, SDRs, or L1b) and derived products (Environmental Data Records, EDR, or L2) from VIIRS, including the sea surface temperature (SST) retrieved from clear-sky ocean brightness temperatures (BTs) in its AVHRR-like window bands.

Since May 2008, SST products at NESDIS have been operationally produced from NOAA and Metop AVHRRs using the Advanced Clear-Sky Processor for Oceans system (ACSPO) [*Liang et al., 2009*; *Petrenko et al., 2010*; *Liang and Ignatov, 2011*]. ACSPO identifies clear-sky ocean pixels and generates SST and aerosol products from corresponding radiances. The Community Radiative Transfer Model (CRTM) [*Han et al., 2006; Chen et al., 2012a,b*] is employed in ACSPO to simulate top of atmosphere clear-sky BTs, using the National Centers for Environmental

Accepted Article

Prediction Global Forecast System (NCEP GFS) upper air and Reynolds daily first-guess SST fields as inputs. Simulated BTs are used in ACSPO to improve cloud masking and data quality control, and to explore physical SST retrievals, in addition to the current empirical regression algorithms tuned against *in-situ* SSTs. Since January 2012, experimental SST products from S-NPP VIIRS and Terra and Aqua MODIS have also been generated at NESDIS. Stability and cross-platform consistency of VIIRS, MODIS, and AVHRR BTs is critical to ensure stability and continuity of POES, EOS, and JPSS SST products.

Monitoring of IR Clear-Sky Radiances over Oceans for SST [MICROS; www.star.nesdis.noaa.gov/sod/sst/micros; *Liang and Ignatov, 2011*] is a web-based near-real time system established in July 2008 to understand and minimize "model minus observation" (M-O) biases in ACSPO clear-sky ocean BTs and SSTs. MICROS proved instrumental for three major applications, including monitoring satellite radiance as a part of the Global Space-based Inter-Calibration System [gsics.wmo.int; *Goldberg et al., 2011*], validation of CRTM and input fields, and evaluation and improvement of ACSPO SST and clear-sky ocean BT products [*Liang et al., 2009*; *Liu et al., 2010*; *Liang and Ignatov, 2011; Saha et al., 2012*].

Initially, MICROS monitored only AVHRR Global Area Coverage (GAC; 4 km resolution) data from NOAA-16, -17, -18, and Metop-A. NOAA-19 was added following its launch in February 2009, and processing of Metop-A global Full Resolution Area Coverage (FRAC; 1 km) began in December 2009. In February 2010, monitoring of NOAA-17 was discontinued after its AVHRR failed. Following the launch of the VIIRS instrument onboard S-NPP in October 2011, and the opening of the cryoradiator doors on 19 January 2012, monitoring in MICROS commenced on 21 January 2012. Two MODIS instruments onboard Terra and Aqua were added at the same time to

Accepted Article

facilitate cross-platform consistency checks. On 17 September 2012, Metop-B was launched. It was added in MICROS on 19 October 2012, after its cryoradiator doors opened on 16 October 2012.

In December 2008, double differences (DD) were added in MICROS to check clear-sky ocean BTs for stability and cross-platform consistency, using radiative transfer model (RTM) simulations as a "transfer standard". Previously, DDs have been successfully employed to cross-compare the two hyper-spectral instruments, AIRS onboard Aqua and IASI onboard Metop-A [*Aumann and Pagano,* 2008; *Strow et al.,* 2008*; Elliott et al.,* 2009] by building upon earlier RTM modeling efforts in conjunction with SST to check AIRS calibration on orbit [*Hagan and Minnett,* 2003*; Aumann et al.,* 2006]. *Wang et al.* [2010, 2011] explored a different DD implementation, by which AIRS and IASI were cross-evaluated using a wide-band imager onboard geostationary satellites as a "transfer standard." The DD technique is now widely employed in GSICS [*Goldberg et al., 2011*].

In this manuscript, MICROS M-O biases and DDs are analyzed to check AVHRR, MODIS, and VIIRS BTs and SSTs for stability and cross-platform consistency. Satellite data and MICROS processing specifics are described in section 2. M-O biases are defined in section 3. In section 4, MICROS DDs are defined and employed to check various sensors for stability and cross-platform consistency. The critical importance of consistent CRTM simulations for quantitative use of MICROS DDs in GSICS applications is discussed in section 5. Conclusions, ongoing work, and future plans are summarized in section 6.

2. Data processing in MICROS

Accepted Article

Currently, data of AVHRR GAC (NOAA-16, -17, -18, -19, Metop-A and -B) and FRAC (Metop-A and -B), MODIS (Terra and Aqua), and VIIRS (S-NPP) are analyzed in MICROS. (Note that the Metop AVHRRs provide global FRAC data, which are additionally processed by NESDIS on the ground to generate a GAC product, using the algorithms implemented onboard NOAA satellites.) Nadir resolution is 4, 1, and 0.75 km for AVHRR GAC, AVHRR FRAC and MODIS, and VIIRS, respectively. Currently, only three SST bands centered at 3.7 (IR37), 11 (IR11), and 12 µm (IR12) are processed, from all sensors (see Table 1).

INSERT TABLE 1 HERE

MICROS processing is fully automated and runs daily in three steps: 1) ACSPO processing of sensor L1b data into L2 product (including appending cloud flag and calculation of regression SSTs from BTs); 2) statistical analyses of M-O biases and DDs for BTs and SSTs; and 3) publication of their statistical summaries in MICROS web page. If only one computer is employed, end-to-end, then it currently takes more than 24 hours of CPU time to process 24 hours of global data from all these platforms (see Table 2). In particular, the processing of the largest S-NPP VIIRS data stream requires ~17 hrs (of which ACSPO processing takes ~9 hrs and MICROS ~8 hrs), and results in ~90 million clear-sky ocean pixels per night, and approximately the same number per day. Processing of one MODIS stream requires 6.5 hrs and results in ~35 million clear-sky pixels per night/day, whereas processing of one AVHRR FRAC requires 5.5 hrs and results in ~45 million clear sky pixels per night/day. Note that AVHRR FRAC provides more data but is processed faster than MODIS due to the binary format of AVHRR L1b files, whereas the compressed hierarchical data format (HDF) for MODIS L1b files requires more time for Input/Output (I/O) operations.

Accepted Article

Processing one global GAC stream takes only 0.8 hr CPU time (0.4 hr ACSPO + 0.4 hr MICROS), and results in ~3 million clear-sky ocean pixels per night/day.

Both daytime and nighttime data are processed and monitored in MICROS, but only nighttime data are used in this study, to minimize the effect of diurnal cycle and solar reflectance contamination on daytime data [*Liang and Ignatov,* 2010].

INSERT TABLE 2 HERE

3. BT and SST biases

The M-O BT and SST biases are defined as follows [*Liang and Ignatov,* 2011]

$$\Delta BT = M - O = BT_{CRTM} - BT_{SENSOR} \tag{1}$$

$$\Delta SST = SST_{SENSOR} - SST_{REYNOLDS} \tag{2}$$

Here, *SENSOR* denotes AVHRR, MODIS, or VIIRS; *REYNOLDS* is first-guess SST used as input into CRTM [*Reynolds et al., 2007*]; SST_{SENSOR} is ACSPO retrieved SST (at night, multi-channel SST, MCSST, regression algorithm is used).

Biases in Equations (1-2) are calculated in each clear-sky ocean pixel, and then their global statistics are analyzed and displayed in MICROS. For validating sensor radiances and CRTM, robust statistics are preferred over their conventional counterparts, to minimize the effect of small fraction of possible outliers in ACSPO data [*Liang and Ignatov,* 2011]. Therefore, median biases are used here.

Accepted Article

The platforms and sensors currently monitored in MICROS and their global coverage are illustrated in Figure 1, which shows maps of the M-O biases in IR37 for one night of data on 6 December 2012. Cloudy areas (rendered in white) are largely consistent across platforms. In cloud-free areas, M-O biases are shown in color scale. Generally, they are uniform, and close to zero.

INSERT FIGURE 1 HERE

For quantitative analyses, global histograms from data shown in Figure 1 are plotted in Figure 2. Their shape is close to Gaussian. In conjunction with narrow width and the large number of clear-sky ocean pixels (shown in Figure 2 and in Table 2), this suggests that global median M-O biases (also superimposed in Figure 2) are estimated very accurately. M-O biases in IR37 are consistent to within ±0.1 K except for NOAA-18 and Aqua. Note that NOAA-18, -19, Aqua and S-NPP fly close orbits (~1:30 a.m.), whereas Metop-A, -B, and Terra overpass a few hours earlier, at ~9:30-10 p.m. The 9:30 p.m. cluster is expected to be a few hundredths Kelvin warmer than the 1:30 a.m. one due to the diurnal cycle in SST which is not accounted for in current daily Reynolds SST product. NOAA-16 currently overpasses around ~7 a.m./p.m.

INSERT FIGURE 2 HERE

Figure 3 shows the time series of the M-O biases in IR37, for AVHRR GAC data. Each point on the time series is a "nightly" global median M-O bias that is calculated from histograms similar to those shown in Figure 2, each of which is produced from ~2.5 to 3 million clear sky ocean pixels (cf. Figure 2 and Table 2). The time series in Figure 3 were smoothed by a 7-day running filter to minimize the visual effect of temporal noise. (Note that the original non-smoothed time series are also available in MICROS.) M-O biases generally remain positive, in all bands of all platforms,

Accepted Article

during the full monitoring period due to several factors unaccounted for in the model and residual cloud in ACSPO BTs (cf. discussion in [*Liang and Ignatov,* 2011], also summarized in caption to Figure 3).

INSERT FIGURE 3 HERE

A prominent feature of Figure 3 is a strong temporal variability in the M-O biases. Special analyses in [*Liang and Ignatov,* 2011; *Saha et al.,* 2012] have shown that it is mainly due to the unstable Reynolds SST used as input into CRTM. Being due to one root cause, these temporal variations are thus largely coherent between different platforms (except NOAA-16, which apparently is subject to another source of noise, exceeding the noise in Reynolds SST; recall that NOAA-16 is in a twilight orbit now, where scan-line by scan-line calibration may not be accurate, due to Sun impingement on AVHRR calibration black body; Cao et al., 2001) and cancel out when selecting one platform as a reference, and calculating DDs.

4. MICROS Double Differences (DD)

Liang and Ignatov [2011] introduced MICROS DDs and employed them to evaluate stability and cross-platform consistency of BTs and SSTs in AVHRR GAC data from July 2008 to October 2009. Here, these analyses are extended to December 2012. Also, shorter time series from Terra and Aqua MODIS, S-NPP VIIRS, and Metop-B AVHRR (all added in 2012) are preliminarily analyzed and evaluated for stability and cross-platform consistency.

4.1 Double Differences

The DD for BTs and SSTs are defined as follows [*Liang and Ignatov,* 2011]

Accepted Article

$$SAT - REF = SAT[-(M - O)] - REF[-(M - O)] \quad (3)$$

$$SST - REF = SST[REG - REYNOLDS] - REF[REG - REYNOLDS] \quad (4)$$

Here, *SAT* denotes the satellite, which is evaluated against the reference platform, *REF* denotes the reference satellite, and *REG* denotes regression SST generated by ACSPO. DDs are expected to cancel out or minimize systematic errors or instabilities in the "M" terms common to all sensors (arising from e.g. errors in reference SST or GFS profile data, incomplete inputs to CRTM such as missing aerosol, possible systemic biases in the CRTM forward model, and updates in ACSPO processing algorithms), and presumably should rectify the difference between the two corresponding "O" terms, i.e. cross-platform radiance bias which is the GSICS objective [cf. *Aumann and Pagano,* 2008; *Elliott et al.,* 2009].

The MICROS DDs characterize two aspects of radiances: their stability and consistency with the reference platform. Stability of the DDs does not necessarily prove that both sensors are stable, but strongly suggests that this is the case. The confidence increases if several different DD combinations derived from different pairs of sensors are all stable. Stability is best seen on longer time series. Figure 4 shows 4+ years of DDs in IR37 derived from Figure 3, using Metop-A GAC as a reference. Generally, NOAA-17 and -19 are more stable than NOAA-16 and -18. This observation has been already made by *Liang and Ignatov* [2011] using 15 months of data. Here, it is additionally confirmed using longer time series. In particular, DDs are very stable in all AVHRR bands of NOAA-17 and Metop-A, which happen to fly a close mid-morning orbit. This strongly suggests that both sensors are stable. Initially, NOAA-17 was selected as a reference platform, with its AVHRR being the longest living stable sensor in MICROS. After its scan motor failed in February 2010, Metop-A GAC appeared a natural substitute. Note that both these platforms overpass ~10pm and

Accepted Article

therefore may be subject to larger residual of diurnal warming than other sensors monitored in MICROS, but the stability of sensors was deemed of higher priority. Another consideration is the availability of two data streams from Metop satellite – GAC and FRAC. GAC minus FRAC DDs are expected to be zero, but Figure 5 suggests that they are actually in a range from 0.02-0.04K, depending upon AVHRR band. This suggests some residual cloud screening differences between 4km GAC and 1km FRAC (and likely high resolution MODIS and VIIRS) data. Work is underway to reconcile the ACSPO cloud mask for low and high resolution data. NOAA-19 – Metop-A DDs are somewhat less stable. Recall that NOAA-19 overpasses several hours after Metop-A, and the diurnal cycle in SST may contribute. On the other hand, NOAA-18 flies a very close orbit to NOAA-19, but the two platforms show significant relative inconsistencies and instabilities, likely due to some unknown sensor calibration issues with their AVHRRs. NOAA-16 (which flew at ~7 a.m./p.m. in 2012) is even more vulnerable. Overall Figure 4 suggests that DDs offer an excellent potential to check sensors for long-term stability, and this potential is expected to improve if a diurnal cycle is resolved in the first guess SST field. Note that the relative stability may be further quantified e.g. as a temporal root mean squared deviation of corresponding DDs, *Saha et al.* [2012], but this is beyond the objectives of this study.

INSERT FIGURE 4 HERE

When two platforms are stable, then their cross-platform consistency can be further evaluated defined as temporal mean of the DDs time series. Biases may be stable in time, but systematically deviate from zero. For instance, NOAA-17 – Metop-A DDs are ~0 K in IR37, ~+0.05 K in IR11, and -0.03 K in IR12 [*Liang and Ignatov,* 2011], and maybe an order of magnitude larger in some anomalous cases, as will be shown below in this section. Note that the RTM DDs account for

Accepted Article

known differences in sensors' spectral responses (RSR) by calculating sensor-specific M-terms, so that DDs are expected to measure the true cross-platform radiance biases for sensor inter-calibration applications within GSICS. However, DDs are also affected by unknown RSR factors, such as errors in their pre-launch characterization or errors caused by on-orbit degradation. Also, since different platforms overpass at different local times, the diurnal effect in first guess SST should be resolved. Since ACSPO employs daily mean Reynolds SST, this study minimizes the corresponding diurnal biases by using only nighttime data.

The remaining part of this section discusses cross-platform consistency between various AVHRR, MODIS and VIIRS instruments, using a common period in 2012, after MODIS and VIIRS data were added in MICROS. Figure 5 shows DDs in all three IR bands and retrieved SSTs from January to December 2012, and is discussed below. Note that Figure 4 suggests that sensors, which may appear quasi-stable on shorter periods (from several months to a year), may be unstable on longer periods of several years. Therefore, the observations for stability of Metop-B AVHRR, Terra and Aqua MODIS, and S-NPP obtained in this section are preliminary, and should be revisited after longer time series of their data are accumulated in MICROS.

INSERT FIGURE 5 HERE

4.2 AVHRR

The cross-platform biases are well within ±0.1 K for AVHRRs onboard NOAA-18, -19, and Metop-A, in all three window bands. NOAA-16 continues to be unstable and out of family due to its AVHRR calibration problems [*Liang and Ignatov,* 2011]. Initial two months of Metop-B show that its BTs are biased with respect to Metop-A by ~+0.12 K, ~+0.30 K, and -0.06 K in IR37, IR11, and

Accepted Article

IR12, respectively. Preliminary analyses suggest that at least part of these biases may be due to the fact that CRTM coefficients for Metop-B have been calculated inconsistently with Metop-A, and other AVHRRs onboard NOAA platforms. As a result, the two "M" terms in Eq. (1) do not fully cancel out. Joint analyses between NESDIS CRTM, SST and Calibration Teams are currently underway to bring Metop-B back in family. Results of these analyses will be reported elsewhere.

The Metop-B SST was biased warm by ~+0.3 K and out of family for the first month after this platform was added in MICROS in October 2012, because initially, Metop-A regression SST coefficients were used to retrieve Metop-B SST. Once sufficient match-up dataset of Metop-B BTs with in situ SSTs was accumulated, SST coefficients were calculated and implemented in MICROS on 15 November 2012, which brought Metop-B SST back in family.

4.3 VIIRS

VIIRS BTs were added in MICROS on 22 January 2012. On 7 March 2012 the calibration of VIIRS thermal bands was fine tuned (C. Cao and F. DeLuccia, 2012, personal communication). As a result, the BTs in all VIIRS SST bands have increased by ~+0.14 K, generally bringing VIIRS BTs closer in AVHRR family.

Following this calibration adjustment, VIIRS regression SSTs, which were calculated using regression coefficients tuned with "old" BTs and were initially consistent with AVHRR and MODIS SSTs to within ±0.1 K, have increased by +0.11 K taking VIIRS SST out of the AVHRR/MODIS family. It took SST Team a month to accumulate enough match-ups of "new" VIIRS BTs with in situ SSTs, and recalculate MCSST regressions. New coefficients implemented on 3 May 2012 have brought VIIRS SSTs back in family.

Accepted Article

4.4 MODIS

Since MODIS implementation in MICROS on 22 January 2012, BTs in the two longwave bands have been exemplarily consistent between Terra and Aqua, but displaced with respect to AVHRR/VIIRS cluster by ~-0.6 K in IR11 and ~-0.3 K in IR12. Extensive joint analyses between NESDIS SST and CRTM Teams, and NASA MODIS Characterization Support Team (MCST) have been conducted to attribute this anomalous behavior of the MODIS longwave M-O biases. It was concluded that suboptimal MODIS transmittance and spectral coefficients implemented in CRTM v2.02 were the cause. Based on analyses in MICROS and feedback from SST Team, the CRTM Team recalculated the coefficients, and released CRTM v2.10 on 13 September 2012. This new CRTM release was immediately incorporated in ACSPO and MICROS, which brought MODIS BTs in both longwave bands back in AVHRR/MODIS family. Note that both longwave bands remain exemplarily consistent between Terra and Aqua.

Prior to 13 September 2012, IR37 on Terra was in family, whereas on Aqua, it was biased low by ~-0.30 K. After CRTM V2.10 was implemented, the DDs have changed by +0.10 K for Terra (moving it away from family) and by +0.11 K for Aqua (moving it closer to family). As a result, now Terra brackets the AVHRR/VIIRS cluster from above, and Aqua from below. Importantly, the bias of ~0.3 K between Terra and Aqua remains (although reduced by 0.01 K from what it was before 13 September 2012). Note that anomalous behavior of MODIS IR37 was also observed by *Hook et al.* [2007], from ASTER and MODIS analyses over lake validation sites. Both results suggest that the cross-platform bias may be due to some unknown MODIS calibration or spectral characterization issue(s). Currently, MODIS L1b data used in ACSPO are from collection 5 [*Xiong et al.,* 2008, 2009], but our preliminary analyses suggest that the same cross-platform bias remains in

Accepted Article

collection 6. Work between NOAA SST and CRTM Teams and NASA MCST is underway to investigate this anomaly and reconcile Terra and Aqua IR37.

5. The importance of consistent CRTM calculations for quantitative DD analyses

Analyses in section 4 suggest that MICROS DDs are excellent way to track sensors stability. However, their use to quantitatively measure cross-platform consistency for GSICS applications to better than ~0.1 K is sensitive to the consistency of the CRTM coefficients, which remains challenging. Effect of CRTM change on DDs was most dramatic for MODIS instrument, up to 0.6 K in IR11. The exact cause of these large biases in MODIS data remains unknown as of this writing. As mentioned, CRTM v2.10 has fixed errors which took place in v2.02. Coefficients for other platforms and sensors were also updated in the new CRTM release. To quantify the effect of CRTM changes on other sensors, parallel processing with both CRTM versions (2.02 and 2.10) was run offline from 13 September to 11 October 2012. Detailed time series are shown in Figure 6, side by side. Since Metop-B was added on 19 October 2012, its data are not shown in Figure 6.

INSERT FIGURE 6 HERE

In all three bands the effect of CRTM update is smallest for AVHRRs onboard NOAA-16, -18, -19 and Metop-A and S-NPP/VIIRS (~-0.01 K), and most dramatic for Terra and Aqua MODIS, up to 0.54 K in IR11. The test run presented an opportunity to test a new set of SST regression coefficients, re-derived from longer and more consistent match-ups with *in situ* data for different platforms. The bottom panels of Figure 6 show time series show that the new SSTs are generally more consistent across platforms (except NOAA-16, due to its unstable BTs). Figure 6 thus provides a quick empirical sensitivity study of DDs to the CRTM coefficients updates from version to version.

Accepted Article

Current CRTM practice is to only generate CRTM coefficients for new sensors not previously included in CRTM, whereas coefficients for most "old" sensors are saved from the prior CRTM releases. The procedure for CRTM coefficients calculation includes running line-by-line radiative transfer model (LBLRTM) with a set of training atmospheric profiles, including various gaseous constituents. The LBLRTM evolves, and different versions of code may be used to run the forward model. Also, there may be a different set of training profiles used in forward calculations, and various minor gases may be occasionally included or excluded from forward LBLRTM calculations. Subsequently, the "exact" LBLRTM calculations are fit with predefined polynomials to generate CRTM coefficients. There are several fit algorithms, including "ordinary" (ORD) and Planck-weighted (PW) [*Chen et. al,* 2012a*; Liang and Ignatov,* 2011]. The atmospheric profile and gaseous absorption also can be treated in two different ways, Optical Depth in Absorption Space (ODAS) and Optical Depth in Pressure Space (ODPS) [*Chen et. al,* 2012b]. As a result, CRTM coefficients calculated at different times and for different CRTM releases may not be fully consistent. As of this writing, SST and CRTM teams are working together to establish an efficient version control for CRTM coefficients, to recalculate all CRTM coefficients for the new releases using a consistent version of LBLRTM, profiles, absorbing gases, ORD/PW and ODAS/ODPS algorithms, and to ensure a uniform set of CRTM coefficients for all platforms and sensors is used in each and every new CRTM release. This will ensure that every new release will use progressively improved parameterizations. Note that for DD applications accuracy is less critical than consistency.

6. Conclusion and future work

In MICROS, BTs and SSTs are monitored for stability and cross-platform consistency using a DD technique. For the accuracy and temporal stability of satellite SSTs, which are currently

Accepted Article

calculated in ACSPO using empirical regressions tuned against in situ data, stability of the sensor BTs is most critical. Out of all AVHRRs monitored in MICROS, the NOAA-16 has been most unstable, followed by NOAA-18. Further analyses are needed to understand whether these are due to fundamental sensor issues, or are caused by suboptimal calibration algorithms employed in NOAA L1b preprocessing, and can be fixed. On the other hand, Metop-A and NOAA-17 and -19 BTs have been most stable and so are their corresponding SST time series.

S-NPP VIIRS and Terra and Aqua MODIS which were added in January 2012, and Metop-B which was added in October 2012, also proved stable, although these observations are based on shorter monitoring periods. There was a discontinuity in VIIRS time series on 7 March 2012, when the VIIRS IR calibration was fine-tuned. As a result, BTs in all SST bands increased by ~+0.14 K. The DD technique was able to successfully capture this change. Another discontinuity in MICROS time series occurred on 13 September 2012 when CRTM was upgraded from v2.02 to 2.10. This CRTM upgrade most dramatically affected MODIS DDs. There was no change in sensor calibration on that date, but rather CRTM coefficients update. Metop-B shows biases with respect to Metop-A of +0.12 K, +0.30 K, and -0.06 K in IR37, IR11, and IR12, respectively. At least in part, those are due to inconsistent CRTM coefficients between Metop-A and -B. Work is underway to recalculate CRTM coefficients and reconcile. On the other hand, Terra/Aqua MODIS inconsistency of ~0.3 K suggests the need for calibration revision in MODIS Band 20.

The MICROS DDs have an excellent potential to monitor BTs from various sensors for cross-platform consistency for GSICS applications. However, large anomalies in MODIS and Metop-B DDs point out the limitation of the RTM methodology. The DDs do cancel out all *consistent* errors and biases in the "M" term when DD is calculated as difference of two M-O biases

Accepted Article

[*Aumann and Pagano,* 2008; *Strow et al.,* 2008*; Elliott et al.,* 2009]. However, if the "M" term is calculated inconsistently (as it was the case in CRTM v2.02 for both MODIS instruments, and, to a lesser extent, also for S-NPP/VIIRS and Metop-B/AVHRR), then the DDs will measure the difference in the "M" terms, in addition to the difference in the "O" terms. In the MODIS case documented here, the problem was large enough and easy to capture. However, it remains unknown to what extent all "M" terms are now consistent in CRTM v2.10. Note also that RTM DDs should account for spectral differences in the two sensors, but this compensation may progressively degrade for significantly different spectral responses, even though the two bands may be located closely in spectrum, especially in the proximity of strong absorption lines. The DD accuracies achieved in the latest MICROS implementation as shown in Figure 6 are thought to approach the limit of the information potential of the DD technique to reconcile different sensors. SST Team continues working with CRTM Team to improve MICROS DDs by using more accurate and consistent CRTM calculations for various sensors monitored in MICROS. For accurate SST applications using RTM methodologies residual bias reconciliation/correction may thus be needed, on order of a few hundredths to a few tenths of a degree Kelvin. On the other hand, if systematic biases in DDs originate from biases in observed BTs, those will be automatically accounted for in the empirical regression SST algorithms.

We also plan to explore accounting for diurnal variation in first-guess SST to improve DD performance, particularly during the daytime. We are also exploring more accurate, higher resolution first guess SST [*Saha et al.,* 2012] and atmospheric profiles. Future work will also be aimed at including solar reflectance bands in MICROS. The CRTM will be used in conjunction with e.g. the Goddard Chemistry Aerosol Radiation and Transport (GOCART, *Chin et al., 2002*) and the Navy

Accepted Article

Aerosol Analysis and Prediction System (NAAPS, www.nrlmry.navy.mil/aerosol/) 3D analyses fields, to generate first-guess top of atmosphere reflectances, and use them to improve ACSPO cloud mask and evaluate DDs for solar reflectance bands.

BTs in SST bands and ACSPO SSTs from all currently functional AVHRR, MODIS, and VIIRS sensors are routinely monitored in MICROS. We also plan to add complete time series of all (Advanced) Along-Track Scanning Radiometers, (A)ATSRs, onboard the European Remote-Sensing Satellites (ERS) and the Environmental Satellite (ENVISAT), and follow-on SST and Land Surface Temperature Radiometer (SLSTR) onboard future European Sentinel-3. Work is also underway to add geostationary sensors in MICROS, the Spinning Enhanced Visible and Infrared Imager onboard Meteosat Second Generation (MSG/SEVIRI), and the Advanced Baseline Imager onboard future Geostationary Operational Environmental Satellite -R Series (GOES-R/ABI). We also plan to add in MICROS several optional SST bands available on some sensors (e.g., the 8.6 µm band on MODIS and VIIRS, and 8.7 µm band on SEVIRI), and explore their additional utility for cloud masking and SST.

Acknowledgments

This work is supported by the JPSS and GOES-R Program Offices, and NOAA Product System Development and Implementation (PSDI) and Ocean Remote Sensing Programs. Thanks to John Stroup, Boris Petrenko, Korak Saha, Yury Kihai, and John Sapper of NESDIS for contributions to ACSPO and MICROS development, and data collection and processing. Thanks to Quanhua Liu, Paul Van Delst, Yong Chen, David Groff and Fuzhong Weng of NESDIS Joint Center for Satellite Data Assimilation provided CRTM, and Eva Borbas and Chris Moeller of University of Wisconsin-Madison for helpful discussions of CRTM coefficients. Thanks also to Simon Hook of Jet Propulsion

Accepted Article

Laboratory (JPL), Xiaoxiong Xiong of NASA Goddard Space Flight Center, Changyong Cao, Fred Wu, Fangfang Yu of NESDIS, and Tim Hewison of EUMETSAT for helpful discussions. Thanks also go to three anonymous Reviewers of this manuscript and JGR Editor, Dr. Des Barton, for valuable recommendations. The views, opinions, and findings contained in this report are those of the authors and should not be construed as an official NOAA or U.S. Government position, policy, or decision.

References

Aumann, H., S. Broberg, D. Elliott, S. Gaiser, and D. Gregorich (2006), Three years of AIRS radiometric calibration validation using sea surface temperatures. *J. Geophys. Res.*, 111, *D16S90*, doi:10.1029/2005JD006822.

Aumann, H., and T. Pagano (2008), Using AIRS and IASI data to evaluate absolute radiometric accuracy and stability for climate applications. *Proc. SPIE Int. Soc. Opt. Eng.*, 7085, doi:10.1117/12.795225.

Cao, C., X. Xiong, F. DeLuccia, Q. Liu, S. Blonski, D. Pogorzala, and H. Oudrari (2012), VIIRS Sensor Data Record (SDR) User's Guide v.1.01, NOAA Tech. Rept. NESDIS 142. https://cs.star.nesdis.noaa.gov/pub/NCC/UsersGuideVIIRS/VIIRS_SDR_USERS_GUIDE_NOAA_TechReport142.pdf

Cao, C., M. Weinreb, and J. Sullivan, 2001: Solar contamination effects on the infrared channels of AVHRR. *JGR*, **106**, 33,463-33,469.

Chen, Y., F. Weng, Y. Han, and Q. Liu (2012a), Planck weighted transmittance and correction of solar reflection for broadband infrared satellite channels. *J. Atmos. Ocean. Technol.*, 29, 382–396. doi:10.1175/JTECH-D-11-00102.1.

Accepted Article

Chen, Y., Y. Han, and F. Weng (2012b), Comparison of two transmittance algorithms in the Community Radiative Transfer Model: Application to AVHRR. *J. Geophys. Res.*, 117, D06206, doi:10.1029/2011JD016656.

Chin, M., P. Ginoux, S. Kinne, B. N. Holben, B. N. Duncan, R. V. Martin, J. Logan, A. Higurashi, and T. Nakajima (2002), Tropospheric aerosol optical thickness from the GOCART model and comparisons with satellite and sun-photometer measurements. *J. Atmos. Sci.*, *59*, 461-483.

Elliott, D., H. Aumann, L. Strow, and S. Hannon (2009), Two-year Comparison of Radiances from AIRS and IASI. *Proc. SPIE Int. Soc. Opt. Eng.*, **7456**, doi:10.1117/12.826996.

Goldberg, M., G. Ohring, J. Butler, C. Cao, R. Datla, D. Doelling, V. Gärtner, T. Hewison, B. Iacovazzi, D. Kim, T. Kurino, J. Lafeuille, P. Minnis, D. Renaut, J. Schmetz, D. Tobin, L. Wang, F. Weng, X. Wu, F. Yu, P. Zhang, T. Zhu (2011), The Global Space-Based Inter-Calibration System. *Bull. Amer. Meteor. Soc.*, **92**, 467–475.

Hagan, D., and P. Minnett (2003), AIRS Radiance Validation over Oceans from SST Measurements. *IEEE Trans. Geosci. Remote Sens.,* 41, 6, 432-441.

Han, Y., P. van Delst, Q. Liu, F. Weng, B. Yan, R. Treadon, and J. Derber (2006), Community Radiative Transfer Model (CRTM)-Version 1, NOAA Technical Report, NESDIS 122, 40 pp.

Hook, S. J, R. G. Vaughan, H. Tonooka (2007), Absolute Radiometric In-Flight Validation of Mid Infrared and Thermal Infrared Data From ASTER and MODIS on the Terra Spacecraft Using the Lake Tahoe, CA/NV, USA, Automated Validation Site. *IEEE Trans. Geosci. Remote Sens.*, 45, 6, 1798-1807.

Accepted Article

Liang, X., and A. Ignatov (2010), Validation and Improvements of Daytime CRTM Performance Using AVHRR IR 3.7 um Band. *13th AMS Conf. Atm. Radiation, Portland, OR*, https://ams.confex.com/ams/pdfpapers/170593.pdf .

Liang, X., and A. Ignatov (2011), Monitoring of IR Clear-sky Radiances over Oceans for SST (MICROS). *J. Atmos. Ocean. Technol., 28,* doi:10.1175/JTECH-D-10-05023.1.

Liang, X., A. Ignatov, and Y. Kihai (2009), Implementation of the Community Radiative Transfer Model (CRTM) in Advanced Clear-Sky Processor for Oceans (ACSPO) and validation against nighttime AVHRR radiances. *J. Geophys. Res.*, 114, *D06112*, doi:10.1029/2008JD010960.

Liu, Q., X. Liang, Y. Han, P. van Delst, Y. Chen, A. Ignatov, and F. Weng (2009), Effect of out-of-band response in NOAA-16 AVHRR Channel 3B on top-of-atmosphere radiances calculated with the Community Radiative Transfer Model. *J. Atmos. Ocean. Technol*, doi:10.1175/2009JTECHA1259.1.

Petrenko, B., A. Ignatov, Y. Kihai, and A. Heidinger (2010), Clear-sky mask for the Advanced Clear-Sky Processor for Oceans. *J. Atmos. Ocean. Technol.*, 27, 1609–1623.

Reynolds, R. W., T. M. Smith, C. Liu, D. B. Chelton, K. S. Casey, and M. G. Schlax (2007), Daily high-resolution blended analyses for sea surface temperature. *J. Climate*, 20, 5473–5496.

Saha, K., A. Ignatov, X. Liang, and P. Dash (2012), Selecting a first guess SST field as input to forward radiative transfer models. *J. Geophys. Res.*, 117, *C12001*, doi:10.1029/2012JC008384.

Strow, L., S. Hannon, and D. Tobin (2008), AIRS and IASI validation and inter-comparisons with SARTA, 4th Annual Advanced High Spectral Resolution Infrared Observations Workshop,

Accepted Article

EUMETSAT, Darmstadt, Germany, 15–17 Sep 2008, www.ssec.wisc.edu/hsr/meetings/2008/presentations/Larrabee_Strow.pdf .

Reynolds, R., T. Smith, C. Liu, D. Chelton, K. Casey, and M. Schlax (2007), Daily high-resolution blended analyses for sea surface temperature. *J. Climate*, 20, 5473–5496.

Wang, L., X. Wu, Y. Li, S. Sohn, M. Goldberg, and C. Cao (2010), Comparison of AIRS and IASI radiance measurements using GOES imagers as transfer radiometers, *J. Appl. Meteorol. Climatol.*, 49, 478–492, doi:10.1175/2009JAMC2218.1.

Wang, L., M. Goldberg, X. Wu, C. Cao, R. Iacovazzi, F. Yu, and Y. Li (2011), Consistency assessment of AIRS and IASI radiances: Double differences versus simultaneous nadir overpasses, *J. Geophys. Res.*, 116, *D11111*, doi:10.1029/2010JD014988.

Xiong, X., K. Chiang, A. Wu, W. Barnes, B. Guenther, and V. Salomonson (2008), Multiyear On-Orbit Calibration and performance of Terra MODIS Thermal Emissive Bands, *IEEE Trans. Geosci. Remote Sens*, 46, 6, 1790-1803.

Xiong, X., B. Wenny, A. Wu, W. Barnes, and V. Salomonson (2009), Aqua MODIS Thermal Emissive Bands On-Orbit Calibration, Characterization and Performance, *IEEE Trans. Geosci. Remote Sens.*, 47, *3*, 803-814.

Accepted Article

Table Captions

Table 1. SST bands of AVHRR, MODIS and VIIRS currently monitored in MICROS. Work is underway to include monitoring of MODIS and VIIRS optional bands.

Table 2. Average number of clear-sky ocean pixels and processing time for 24 hours of L1b data.

Accepted Article

Figure Captions

Figure 1. Global distributions of nighttime M-O BT biases in IR37 on 6 December 2012 from: (Left panels) AVHRR GAC (Metop-A, -B, NOAA-16, -18, and -19); (Right panels) AVHRR FRAC (Metop-A and -B), MODIS (Terra and Aqua), and VIIRS (S-NPP).

Figure 2. Histograms of M-O BT biases from Figure 1, separately for (left) AVHRR GAC and (right) high-resolution data. Note a near-Gaussian shape (the dotted lines are Gaussian fits corresponding to the median and robust standard deviation), narrow width and close cross-platform consistency, except for Aqua MODIS which is out of family. Histograms are based on very large number of clear-sky ocean pixels (from 2.5 to 2.9 million for AVHRR GAC, and from ~37 to ~96 million for high resolution data), resulting in a very accurate estimate of the global median M-O biases. A positive bias for all platforms and sensors is due to missing aerosol in CRTM input; using daily average bulk Reynolds SST (instead of diurnal-cycle adjusted nighttime skin SST); and residual cloud contamination in ACSPO clear-sky BTs.

Figure 3. Time series of global nighttime M-O biases in IR37 from AVHRR GAC (NOAA-16, -17, -18, -19 and Metop-A). Note that M-O biases change in time, due to instabilities in both model and sensor BTs. However, different platforms closely track each other, due to the common origin of model errors resulting from temporal instability of the Reynolds SST [*Liang and Ignatov,* 2011; *Saha et al.,* 2012].

Figure 4. Time series of Double Differences (DD) derived from Fig. 3. Metop-A GAC is selected as a reference platform. Note that NOAA-17 overpass time is close to that of Metop-A @9:30 p.m.. The two platforms are very consistent, as expected. NOAA-18 and -19 overpass at ~1:30 a.m. and are also expected to be consistent, being slightly cooler than Metop-A and NOAA-17, due to the diurnal cycle in SST. However, they are inconsistent with each other, and NOAA-18 is warmer than NOAA-17 and Metop-A. NOAA-16 observation time drifted from 4-7 a.m. over a 4-year period, and its AVHRR measurements are very unstable, most likely due to the twilight orbit affecting its calibration.

Accepted Article

Figure 5. Double-differences in IR37, IR11, IR12, and SSTs for NOAA-16, -18 and -19 AVHRR GAC, Metop-A FRAC, Terra and Aqua MODIS, and S-NPP VIIRS from January 2012 onward. Each point is calculated from all nighttime clear-sky pixels over global ocean, over 24-hour interval.

Figure 6. Same as in Fig. 5 but from 13 September to 11 October 2012. (Left panels): Calculated with CRTM v2.02. (Right panels): Calculated using CRTM v2.10 released on 14 September 2012.

Accepted Article

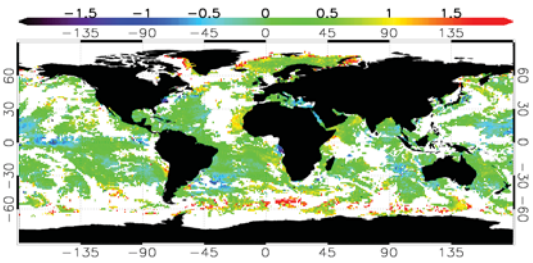

Median(CRTM−OBS, K), AVHRR−METOPA IR37, 2012−12−06(Night)

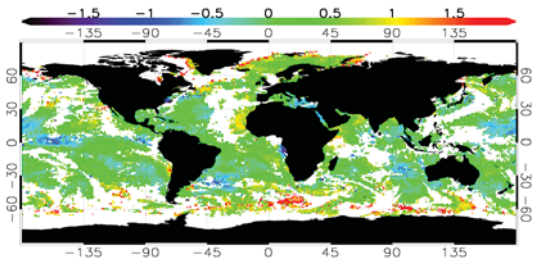

Median(CRTM−OBS, K), AVHRR−MAFRAC IR37, 2012−12−06(Night)

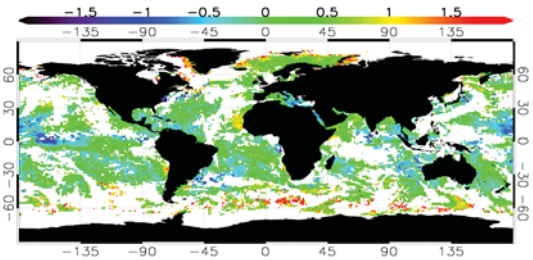

Median(CRTM−OBS, K), AVHRR−METOPB IR37, 2012−12−06(Night)

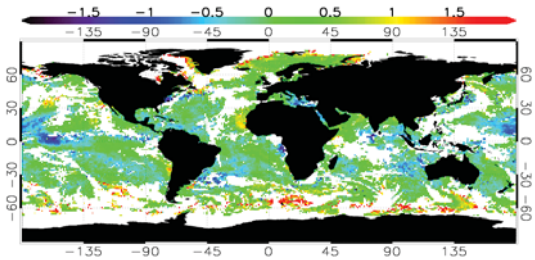

Median(CRTM−OBS, K), AVHRR−MBFRAC IR37, 2012−12−06(Night)

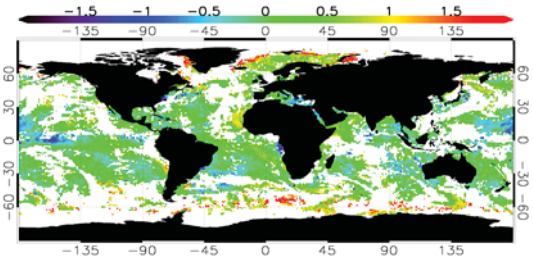

Median(CRTM−OBS, K), AVHRR−NOAA16 IR37, 2012−12−06(Night)

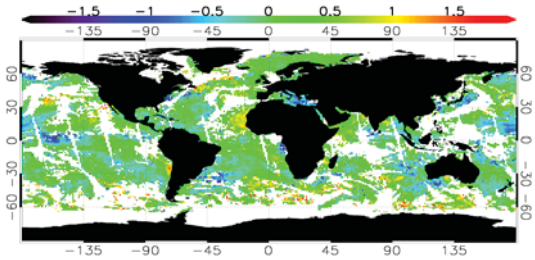

Median(CRTM−OBS, K), MODIS−TERRA IR37, 2012−12−06(Night)

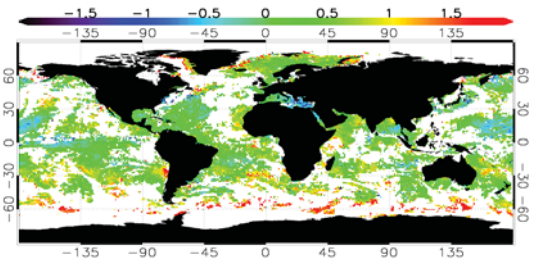

Median(CRTM−OBS, K), AVHRR−NOAA18 IR37, 2012−12−06(Night)

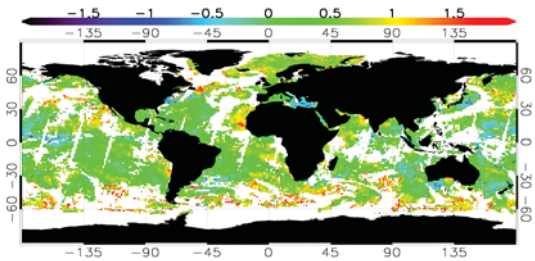

Median(CRTM−OBS, K), MODIS−AQUA IR37, 2012−12−06(Night)

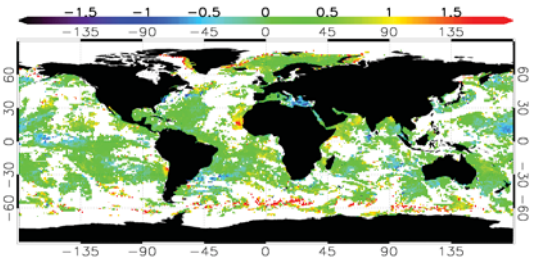

Median(CRTM−OBS, K), AVHRR−NOAA19 IR37, 2012−12−06(Night)

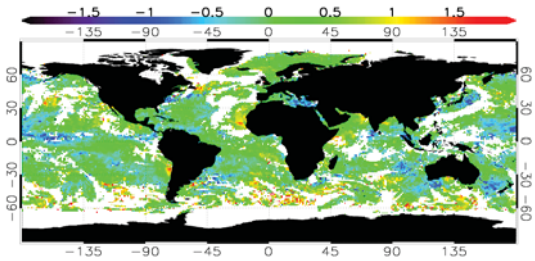

Median(CRTM−OBS, K), VIIRS−NPP IR37, 2012−12−06(Night)

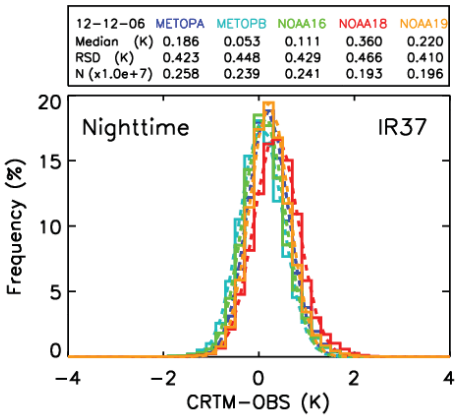

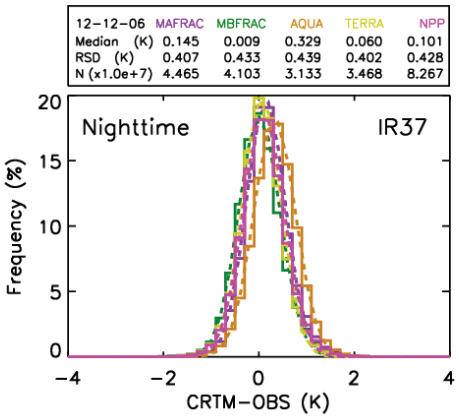

Accepted Article

Accepted Article

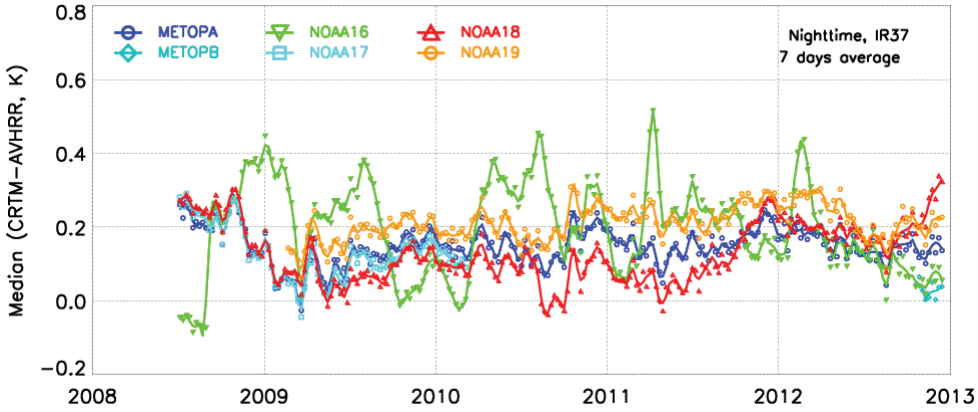

Accepted Article

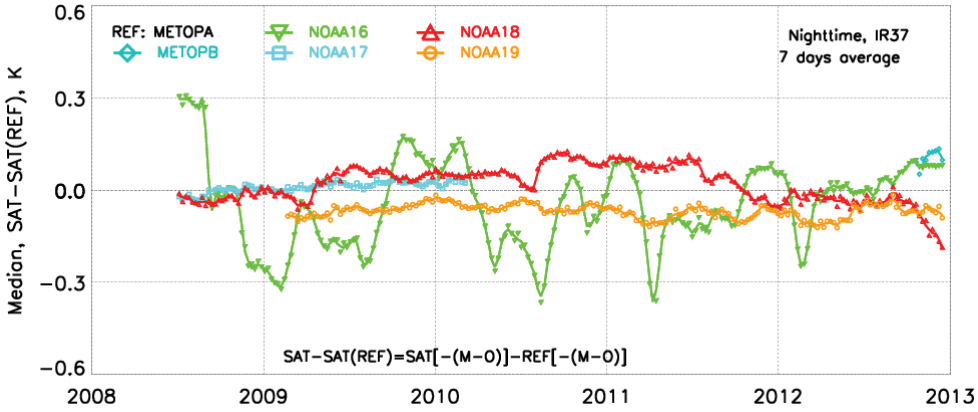

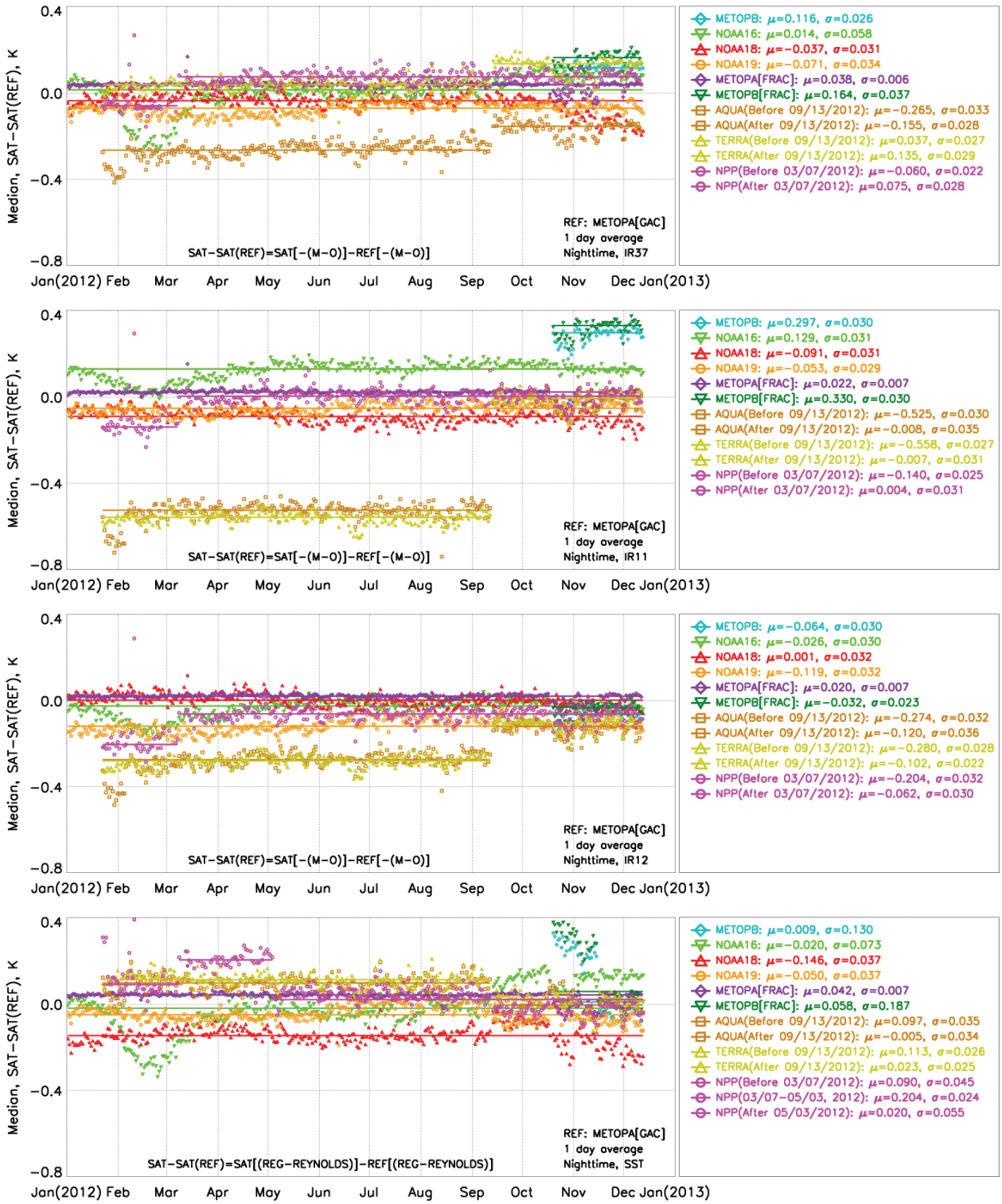
Median, SAT−SAT(REF), K
0.4
0.0
−0.4
−0.8
Jan(2012) Feb Mar Apr May Jun Jul Aug Sep Oct Nov Dec Jan(2013)
SAT−SAT(REF)=SAT[−(M−O)]−REF[−(M−O)]
REF: METOPA[GAC]
1 day average
Nighttime, IR37
METOPB: μ=0.116, σ=0.026
NOAA16: μ=0.014, σ=0.058
NOAA18: μ=−0.037, σ=0.031
NOAA19: μ=−0.071, σ=0.034
METOPA[FRAC]: μ=0.038, σ=0.006
METOPB[FRAC]: μ=0.164, σ=0.037
AQUA(Before 09/13/2012): μ=−0.265, σ=0.033
AQUA(After 09/13/2012): μ=−0.155, σ=0.028
TERRA(Before 09/13/2012): μ=0.037, σ=0.027
TERRA(After 09/13/2012): μ=0.135, σ=0.029
NPP(Before 03/07/2012): μ=−0.060, σ=0.022
NPP(After 03/07/2012): μ=0.075, σ=0.028
Median, SAT−SAT(REF), K
0.4
0.0
−0.4
−0.8
Jan(2012) Feb Mar Apr May Jun Jul Aug Sep Oct Nov Dec Jan(2013)
SAT−SAT(REF)=SAT[−(M−O)]−REF[−(M−O)]
REF: METOPA[GAC]
1 day average
Nighttime, IR11
METOPB: μ=0.297, σ=0.030
NOAA16: μ=0.129, σ=0.031
NOAA18: μ=−0.091, σ=0.031
NOAA19: μ=−0.053, σ=0.029
METOPA[FRAC]: μ=0.022, σ=0.007
METOPB[FRAC]: μ=0.330, σ=0.030
AQUA(Before 09/13/2012): μ=−0.525, σ=0.030
AQUA(After 09/13/2012): μ=−0.008, σ=0.035
TERRA(Before 09/13/2012): μ=−0.558, σ=0.027
TERRA(After 09/13/2012): μ=−0.007, σ=0.031
NPP(Before 03/07/2012): μ=−0.140, σ=0.025
NPP(After 03/07/2012): μ=0.004, σ=0.031
Median, SAT−SAT(REF), K
0.4
0.0
−0.4
−0.8
Jan(2012) Feb Mar Apr May Jun Jul Aug Sep Oct Nov Dec Jan(2013)
SAT−SAT(REF)=SAT[−(M−O)]−REF[−(M−O)]
REF: METOPA[GAC]
1 day average
Nighttime, IR12
METOPB: μ=−0.064, σ=0.030
NOAA16: μ=−0.026, σ=0.030
NOAA18: μ=0.001, σ=0.032
NOAA19: μ=−0.119, σ=0.032
METOPA[FRAC]: μ=0.020, σ=0.007
METOPB[FRAC]: μ=−0.032, σ=0.023
AQUA(Before 09/13/2012): μ=−0.274, σ=0.032
AQUA(After 09/13/2012): μ=−0.120, σ=0.036
TERRA(Before 09/13/2012): μ=−0.280, σ=0.028
TERRA(After 09/13/2012): μ=−0.102, σ=0.022
NPP(Before 03/07/2012): μ=−0.204, σ=0.032
NPP(After 03/07/2012): μ=−0.062, σ=0.030
Median, SAT−SAT(REF), K
0.4
0.0
−0.4
−0.8
Jan(2012) Feb Mar Apr May Jun Jul Aug Sep Oct Nov Dec Jan(2013)
SAT−SAT(REF)=SAT[(REG−REYNOLDS)]−REF[(REG−REYNOLDS)]
REF: METOPA[GAC]
1 day average
Nighttime, SST
METOPB: μ=0.009, σ=0.130
NOAA16: μ=−0.020, σ=0.073
NOAA18: μ=−0.146, σ=0.037
NOAA19: μ=−0.050, σ=0.037
METOPA[FRAC]: μ=0.042, σ=0.007
METOPB[FRAC]: μ=0.058, σ=0.187
AQUA(Before 09/13/2012): μ=0.097, σ=0.035
AQUA(After 09/13/2012): μ=−0.005, σ=0.034
TERRA(Before 09/13/2012): μ=0.113, σ=0.026
TERRA(After 09/13/2012): μ=0.023, σ=0.025
NPP(Before 03/07/2012): μ=0.090, σ=0.045
NPP(03/07−05/03, 2012): μ=0.204, σ=0.024
NPP(After 05/03/2012): μ=0.020, σ=0.055

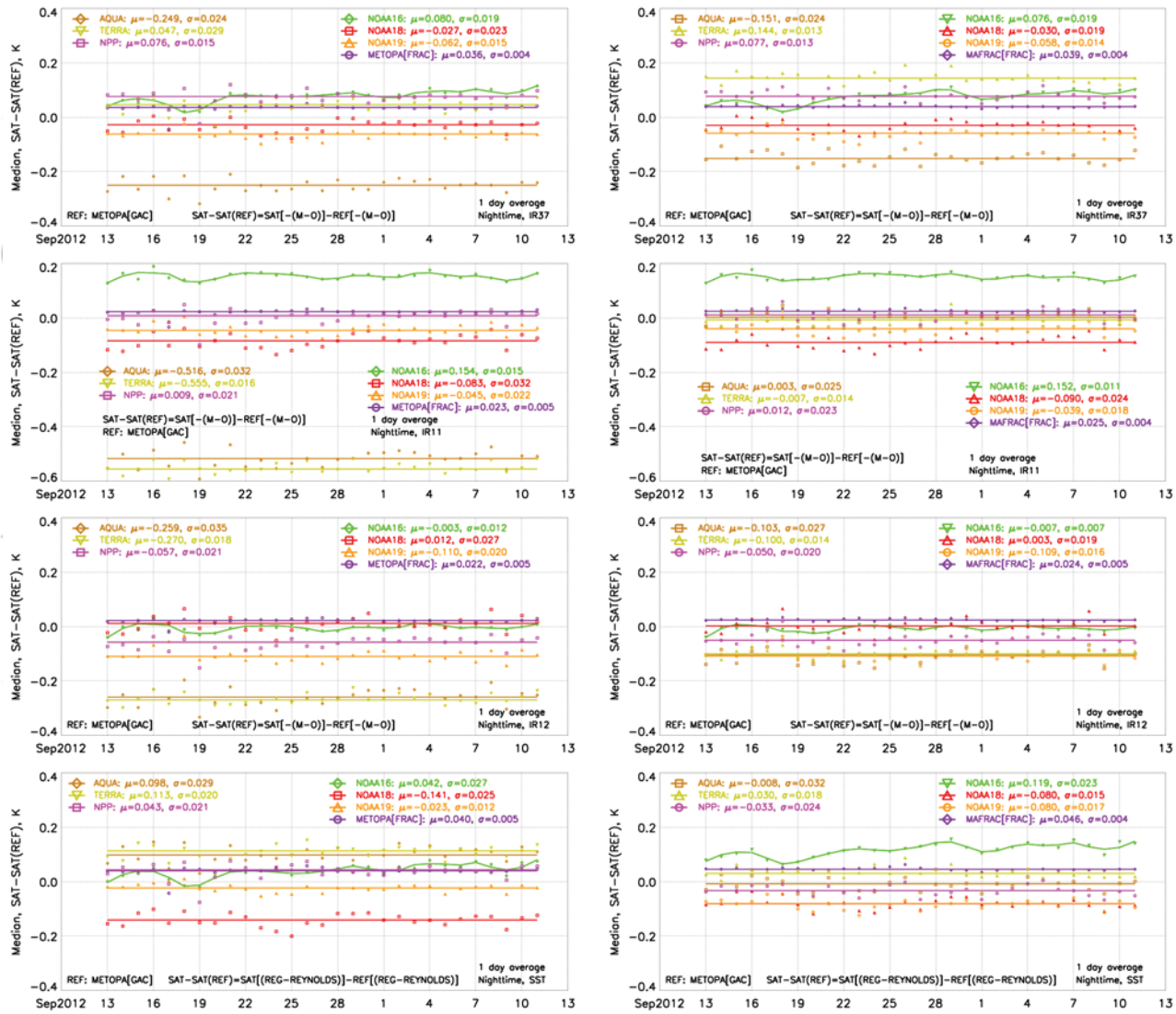
AQUA: μ=−0.249, σ=0.024
TERRA: μ=0.047, σ=0.029
NPP: μ=0.076, σ=0.015
NOAA16: μ=0.080, σ=0.019
NOAA18: μ=−0.027, σ=0.023
NOAA19: μ=−0.062, σ=0.015
METOPA[FRAC]: μ=0.036, σ=0.004
REF: METOPA[GAC]
SAT−SAT(REF)=SAT[−(M−O)]−REF[−(M−O)]
1 day average
Nighttime, IR37
AQUA: μ=−0.151, σ=0.024
TERRA: μ=0.144, σ=0.013
NPP: μ=0.077, σ=0.013
NOAA16: μ=0.076, σ=0.019
NOAA18: μ=−0.030, σ=0.019
NOAA19: μ=−0.058, σ=0.014
MAFRAC[FRAC]: μ=0.039, σ=0.004
REF: METOPA[GAC]
SAT−SAT(REF)=SAT[−(M−O)]−REF[−(M−O)]
1 day average
Nighttime, IR37
AQUA: μ=−0.516, σ=0.032
TERRA: μ=−0.555, σ=0.016
NPP: μ=0.009, σ=0.021
NOAA16: μ=0.154, σ=0.015
NOAA18: μ=−0.083, σ=0.032
NOAA19: μ=−0.045, σ=0.022
METOPA[FRAC]: μ=0.023, σ=0.005
SAT−SAT(REF)=SAT[−(M−O)]−REF[−(M−O)]
REF: METOPA[GAC]
1 day average
Nighttime, IR11
AQUA: μ=0.003, σ=0.025
TERRA: μ=−0.007, σ=0.014
NPP: μ=0.012, σ=0.023
NOAA16: μ=0.152, σ=0.011
NOAA18: μ=−0.090, σ=0.024
NOAA19: μ=−0.039, σ=0.018
MAFRAC[FRAC]: μ=0.025, σ=0.004
SAT−SAT(REF)=SAT[−(M−O)]−REF[−(M−O)]
REF: METOPA[GAC]
1 day average
Nighttime, IR11
AQUA: μ=−0.259, σ=0.035
TERRA: μ=−0.270, σ=0.018
NPP: μ=−0.057, σ=0.021
NOAA16: μ=−0.003, σ=0.012
NOAA18: μ=0.012, σ=0.027
NOAA19: μ=−0.110, σ=0.020
METOPA[FRAC]: μ=0.022, σ=0.005
REF: METOPA[GAC]
SAT−SAT(REF)=SAT[−(M−O)]−REF[−(M−O)]
1 day average
Nighttime, IR12
AQUA: μ=−0.103, σ=0.027
TERRA: μ=−0.100, σ=0.014
NPP: μ=−0.050, σ=0.020
NOAA16: μ=−0.007, σ=0.007
NOAA18: μ=0.003, σ=0.019
NOAA19: μ=−0.109, σ=0.016
MAFRAC[FRAC]: μ=0.024, σ=0.005
REF: METOPA[GAC]
SAT−SAT(REF)=SAT[−(M−O)]−REF[−(M−O)]
1 day average
Nighttime, IR12
AQUA: μ=0.098, σ=0.029
TERRA: μ=0.113, σ=0.020
NPP: μ=0.043, σ=0.021
NOAA16: μ=0.042, σ=0.027
NOAA18: μ=−0.141, σ=0.025
NOAA19: μ=−0.023, σ=0.012
METOPA[FRAC]: μ=0.040, σ=0.005
REF: METOPA[GAC]
SAT−SAT(REF)=SAT[(REG−REYNOLDS)]−REF[(REG−REYNOLDS)]
1 day average
Nighttime, SST
AQUA: μ=−0.008, σ=0.032
TERRA: μ=0.030, σ=0.018
NPP: μ=−0.033, σ=0.024
NOAA16: μ=0.119, σ=0.023
NOAA18: μ=−0.080, σ=0.015
NOAA19: μ=−0.080, σ=0.017
MAFRAC[FRAC]: μ=0.046, σ=0.004
REF: METOPA[GAC]
SAT−SAT(REF)=SAT[(REG−REYNOLDS)]−REF[(REG−REYNOLDS)]
1 day average
Nighttime, SST
Median, SAT−SAT(REF), K
Sep2012 13 16 19 22 25 28 1 4 7 10 13

Accepted

Table 1. SST bands of AVHRR, MODIS and VIIRS currently monitored in MICROS. Work is underway to include monitoring of MODIS and VIIRS optional bands.

Sensor	IR37		IR11		IR12		Optional	
AVHRR	Ch3B	3.74 µm	Ch4	10.80 µm	Ch5	12.00 µm	N/A	N/A
MODIS	Ch20	3.79 µm	Ch31	11.02 µm	Ch32	12.03 µm	Ch22 Ch23 Ch29	3.96 µm 4.06 µm 8.52 µm
VIIRS	M12	3.70 µm	M15	10.76 µm	M16	12.01 µm	M13 M14	4.05 µm 8.55 µm

Accepted Article

Table 2. Average number of clear-sky ocean pixels and processing time for 24 hours of L1b data.

	5 AVHRR GAC (NOAA-16,-18,-19, Metop-A and -B)	2 AVHRR FRAC (Metop-A & -B)	2 MODIS (Terra & Aqua)	1 VIIRS (S-NPP)
umber of Clear Ocean Pixels per night / day	~3M × 5	~45M × 2	~35M × 2	~90M × 1
Total CPU Hours = ACSPO + MICROS	4 = 2 + 2	11 = 7 + 4	13 = 9 + 4	17 = 9 + 8

Accepted Article